

# Estimation of the pole tide gravimetric factor at the chandler period through wavelet filtering

X.-G. Hu,<sup>1</sup> L.-T. Liu,<sup>1</sup> B. Ducarme,<sup>2</sup> H. J. Xu<sup>1</sup> and H.-P. Sun<sup>1</sup>

<sup>1</sup>Institute of Geodesy and Geophysics, Chinese Academy of Sciences, 340 Xu-Dong Road, Wuhan, China. E-mail: hxg432@sohu.com

<sup>2</sup>Research Associate NFSR, Royal Observatory of Belgium, Av. Circulaire 3, B-1180, Brussels, Belgium

Accepted 2006 December 12. Received 2006 October 13; in original form 2006 February 9

## SUMMARY

Wavelet analysis for filtering is used to improve estimation of gravity variations induced by Chandler wobble. This method eliminate noise in superconducting gravimeter (SG) records with bandpass filters derived from Daubechies wavelet. The SG records at four European stations (Brussels, Membach, Strasbourg and Vienna) are analysed in this study. First, the earth tidal constituents are removed from the observed data by using synthetic tides, then the gravity residuals are filtered into a narrow period band of 256–512 d by a wavelet bandpass filter. These data are submitted to three regression analysis methods for estimating the gravimetric factor of the Chandler wobble. After processing by wavelet filtering, SG records can provide amplitude factors  $\delta$  and phase lags  $\kappa$  of the Chandler wobble with much smaller mean square deviation (MSD) than these provided by former studies. It is mainly because the wavelet method can effectively eliminate instrumental drift and provide smoothed data series for the regression analysis.

**Key words:** Chandler wobble, pressure correction, superconducting gravimeter, wavelet filter.

## 1 INTRODUCTION

Variations in the geocentric position of the rotation axis (i.e. polar motion) of the earth will perturb the centrifugal force and thus deform the Earth. Polar motion consists of two main frequency components: the Chandler wobble and the forced annual wobble at period about 432 and 365 d, respectively. Modern space geodetic observation techniques, such as very long baseline interferometer (VLBI) and global positioning system (GPS), can now observe the temporal variations of earth orientation parameters (EOP) with an accuracy less than 1 mas (1 mas = 1 milli-arcsecond). The time-dependent Earth deformation induced by the Polar motion can affect high-precise gravity observations. The superconducting gravimeter (SG) is the world's most sensitive and stable gravimeter. With a sensitivity of  $0.01 \text{ nm s}^{-2}$  and instrument drift less than a few  $10 \text{ nm s}^{-2}$  per year, the SG is able to observe gravity effects caused by the polar motion, the so-called 'pole tide'. The pioneering work of study of the polar motion using SG records goes back to Richter & Zürn (1988). After them some challenging studies to investigate the nature of the gravity variations caused by the polar motion using SG and EOP data have been conducted (De Meyer & Ducarme 1991; Richter *et al.* 1995; Sato *et al.* 1997; Loyer *et al.* 1999; Sato *et al.* 2001; Xu *et al.* 2004; Harnisch & Harnisch 2006).

However, all the above mentioned previous works brings out several points worthy of further consideration. First, the instrumental drift is usually approximated by polynomial or exponential model over the entire observation intervals. Such an approximation is ef-

fective when the drift is continuous but it certainly fails when SG measurement has jumps or discontinuities, the observation from SG T003 at the station Brussels is such a case (Ducarme *et al.* 2005). Secondly, Because of no efficient narrow bandpass filter in previous works, the annual and Chandler components in SG records are usually filtered into a comparatively wide frequency band in which there still exist large, complicated long-period regional perturbations which can be hardly removed by mathematical models and may affect the estimation of the gravimetric factors of the pole tide. Furthermore, some previous studies used the same atmospheric pressure correction in the pole tide analysis as in the Earth tidal analysis at daily and subdaily period, that is, correction with a mean barometric admittance over whole frequency range. However many studies proved that the admittance was obviously frequency-dependent and that its value at low frequency was significantly smaller than the mean value (e.g. Crossley *et al.* 1995; Neumeyer 1995; Hu *et al.* 2005, 2006b). The gravity residuals in the pole tide band could thus be overcorrected if a mean local barometric admittance is used in the pressure correction.

The main motivation behind this study is to try to solve the problems quoted above with wavelet filtering method.

In the following Section 2, we simply introduce the rationale of the wavelet filtering method. In Section 3, SG records from four European stations are processed to obtain gravity residuals, and theoretical pole tides are computed from IERS data. Then in Section 4, the wavelet filtering is applied on gravity residuals to eliminate instrumental drift and other noise. Section 5 estimates the gravimetric

factor of pole tide at Chandler frequency by using three regression analysis methods. Finally, the results of different methods and authors are compared and discussed in Section 6, together with additional considerations on the pressure correction.

## 2 WAVELET FILTERING METHOD

It is well known that a Fourier analysis expands a signal  $f(t)$  in terms of sines and cosines. The signal can also be decomposed into a weighted sum of different wavelets derived from dilation and translation of two closely related basic functions, scaling function  $\phi(t)$  and analysing wavelet  $\psi(t)$

$$f(t) = \sum_n a_j(n) 2^{j/2} \phi(2^j t - n) + \sum_{j=1}^J \sum_{n=0}^{2^j-1} d_j(n) 2^{j/2} \psi(2^j t - n), \quad (1)$$

where  $J$ ,  $j$  and  $n$  are integer indices. The dilation  $2^j$  allows the characterization of the frequency contents of the signal while the translation  $n$  enables the localization of different frequency content in time-space (e.g. Mallat 1989a,b; Daubechies 1992). Decomposition coefficients  $d_j(n)$  are known as the dyadic discrete wavelet transform of the signal and they reflect high frequency variations of the signal, and coefficients  $a_j(n)$  are approximation coefficients of the signal at scale  $2^{-j}$  and they reflect low frequency variations of the signal. These decomposition coefficients are implemented efficiently using a pyramid algorithm, a remarkably fast algorithm that involves low- and high-pass filtering along with a downsampling (decimation) or up-sampling (zero-padding) operator (Mallat 1989a).

With different scale index  $J$ ,  $a_j(n)$  and  $d_j(n)$  are different. So eq. (1) is the multiresolution decomposition that represents characteristics of the signal at different resolutions (Mallat 1989b). In wavelet decomposition, each scale index  $j$  roughly corresponds to a period band:

$$[2^j \Delta t, 2^{j+1} \Delta t], j = 1, 2, \dots, J, \quad (2)$$

where  $\Delta t$  is the sampling interval of the signal. Thus, wavelet transform is actually parallel bandpass filtering. We can select appropriate wavelet to make the wavelet filter adapt to the signal to get better filtering performance. The Daubechies wavelet (Daubechies 1988) is effective for extracting harmonics in signals because it is a compact support (i.e. non-zero only over a finite-region) and orthogonal wavelet.

In processing gravity time-series, the Daubechies wavelet filter have the following advantages over conventional Finite Impulse Response (FIR) filters: filtering signal into very narrow band with good frequency response, exhibiting no Gibbs-like phenomenon and causing no energy loss and phase shift (Hu *et al.* 2005, 2006a,b). The Daubechies wavelet filters can suppress polynomial component in signals. It is due to the vanishing moment property of Daubechies wavelets. A Daubechies wavelet  $\psi(t)$  with support size of  $2p - 1$  has  $p$  vanishing moments if

$$\int_{-\infty}^{+\infty} t^k \psi(t) dt = 0, \text{ for } k = 0, 1, \dots, p - 1. \quad (3)$$

This means that  $\psi(t)$  is orthogonal to any polynomials of degree  $p - 1$ . Thus it is clear that Daubechies wavelet filtering lead to the cancellation of polynomial components up to degree  $p - 1$ . This property is used to eliminate the SG drift. The SG drift, even with jumps or discontinuities, can be suppressed thoroughly without need of any mathematical model and the harmonic components of SG records are smoothly represented.

## 3 DATA PROCESSING

Data series from four SG stations (Brussels, Membach, Strasbourg and Vienna), were collected from the GGP database (Crossley *et al.* 1999). We start from the uncorrected ‘minute data’ in the database. Before the SG data series are used for the study of pole tide, their spikes, gaps, steps and large amplitude caused by earthquake are corrected using T-soft; a graphical and interactive software developed by Van Camp and Vauterin (Vauterin 1988; Van Camp & Vauterin 2005). To maintain the long-term trend of the data, the steps in SG records should be carefully handled. After correction, the minute data series are resampled to hourly data series without using any filter.

The gravity residuals are obtained by subtraction of synthetic earth tides, which are computed using the Tamura potential (Tamura 1987) and tidal parameters compute with the tidal analysis program VAV (Venedikov *et al.* 2001, 2003). The gravity residuals are resampled again to daily data series, and still no filtering techniques are applied (see Fig. 1).

Theoretically for a rigid Earth, the gravity variations induced by polar motion can be predicted by

$$p_{\text{rigid}}(t) = R\Omega^2 \sin 2\theta [x(t) \cos \lambda + y(t) \sin \lambda] \quad (4)$$

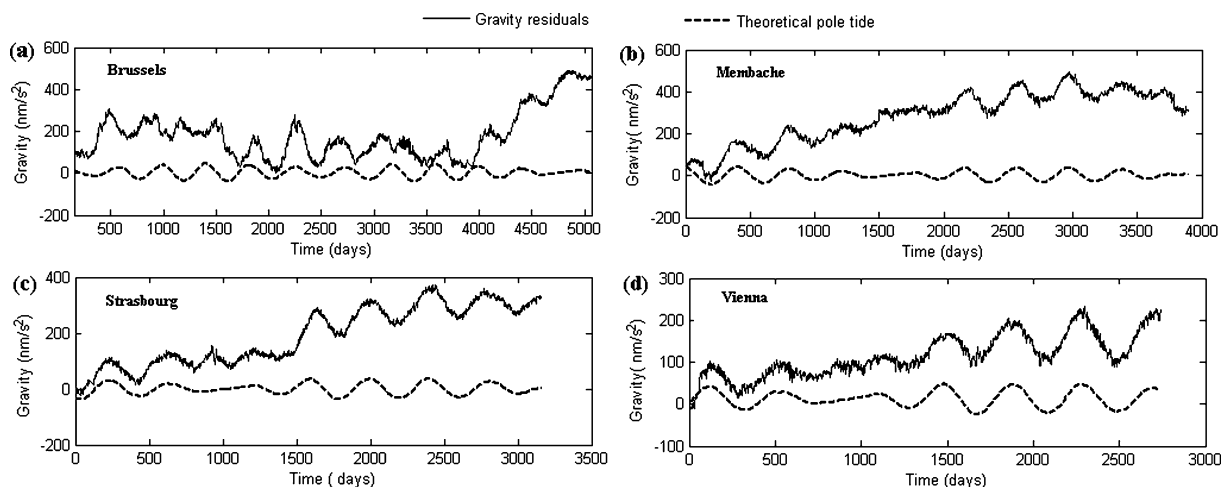


Figure 1. Gravity residuals and theoretical pole tides at station (a) Brussels, (b) Membach, (c) Strasbourg and (d) Vienna.

(e.g. Kaneko *et al.* 1974; Wahr 1985; Capitaine 1986; Hinderer & Legros 1989), where  $R(6.371 \times 10^6 \text{ m})$  is the mean geocentric radius,  $\Omega(7.292115 \times 10^{-5} \text{ rad s}^{-1})$  is the mean angular velocity of the Earth, and  $\theta$  and  $\lambda$  are the colatitude and west longitude of the observation site, respectively.  $x(t)$  and  $y(t)$ , expressed in arcseconds, are the instantaneous pole coordinates in the Celestial Ephemeris Pole relative to the International Reference Pole. Here we use polar motion data set EOPC04 and eq. (4) to determine theoretical pole tides at SG stations. EOPC04 is a smoothed EOP data set provided by IERS (International Earth Rotation Service), derived on a one-day basis, at midnight (00.00 hr UTC), from VLBI, Lunar Laser Ranging (LLR), Satellite Laser Ranging (SLR) and GPS measurements. Theoretical pole tides at the four SG stations are shown in Fig. 1.

#### 4 WAVELET FILTERING OF GRAVITY RESIDUALS

The upward trend of gravity residuals in Fig. 1 comes from the instrumental drift of SG and some real long-term gravity variations. Usually in tidal gravity analysis the instrumental drift of SG is described by polynomials, such as linear or quadratic drift model. When the SG data series covers several years, a simple mathematical function sometimes is not sufficient because the SG drift can hardly remain a perfectly continuous function (without jump and rapid behaviour changes). The SG measurement at station Brussels is a typical case.

In order to eliminate the instrumental drift, we filter gravity residuals into a very narrow subband  $1/2^8 \sim 1/2^7$  cpd, that is, period 256 to 512 d, by using a Daubechies wavelet filter. Thus noise outside this band is removed, including instrument drift and high frequency noise. The same is done with the set of theoretical gravity data, derived from the observed polar motion and eq. (4). The local barometric measurements are also filtered in the same way in order to estimate atmospheric effects in the pole tidal band.

After subtraction of the instrumental drift, the remaining residues oscillate around the zero line. This signal is mainly caused by the superposition of the influence of the annual and Chandler wobble. Fig. 2 shows that the observed pole tide corresponds quite well to the theoretical pole tide at the station Membach, Strasbourg and Vienna, which means the gravity effect of the polar motion is nearly

completely represented by the recorded gravity. The station Brussels is an exception due to its extra large annual noise (see Fig. 3).

To check cleaning capabilities of the wavelet method, we compare the filtered gravity residuals with unfiltered ones at the four stations in the frequency domain. The spectra in Fig. 3 show that long-period components are clearly removed after wavelet filtering but the polar motion signal is unaffected. We can also see from Fig. 3 that there are large annual signal at the stations Brussels and Strasbourg. In Strasbourg and Vienna the annual component is not separable. Besides the annual wobble effect, the anomalous annual signal could be due to the global annual variations in the sea level, atmosphere, hydrology cycle and other annual geophysical effects, but until now most of these effects have not yet been accurately modelled. Moreover, the instrumental reactions to meteorological effects are very complex and could trigger large annual variations in the measurement, such as the effect of annual temperature variation of the room where the SG is located and the effect of annual tilt variation (the Brussels instrument was not tilt compensated).

#### 5 REGRESSION ANALYSIS

To estimate the amplitude factor  $\delta$  and phase difference  $\kappa$  of Chandler wobble, we have to separate the chandler constituent from the annual one. In the following, three separation methods are described. The measurement from the station Membach is taken as an example to give some detail demonstration.

##### 5.1 Fitting sinusoidal functions to the pole tide

Least-squares fitting of two sinusoidal functions with period 432 and 365.25 d to the pole tide in the time domain is a usual method to separate the Chandler component from the annual one (e.g. Xu *et al.* 2004; Harnisch & Harnisch 2006).

After wavelet filtering of SG data, the regression adjustment becomes quite easy as not much environmental noise is left in the period band 256–512 d. The data series in the period band 256–512 d can be simply modelled as sum of two sinusoidal functions

$$\Delta g_1(t) = \sum_{i=1}^2 A_i \cos(\omega_i t + a_i) + C \cdot P(t, \Delta T), \quad (5)$$

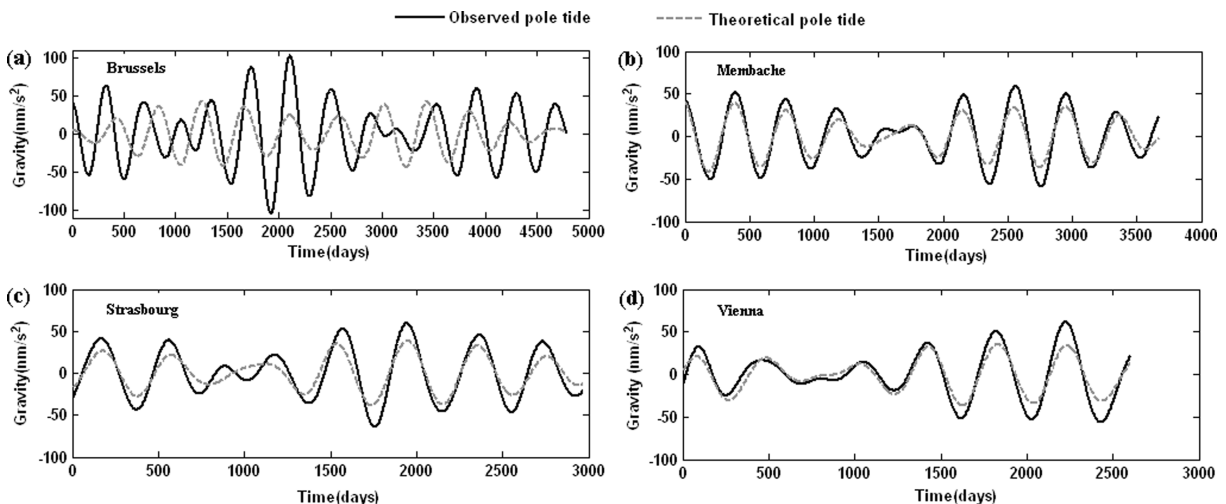
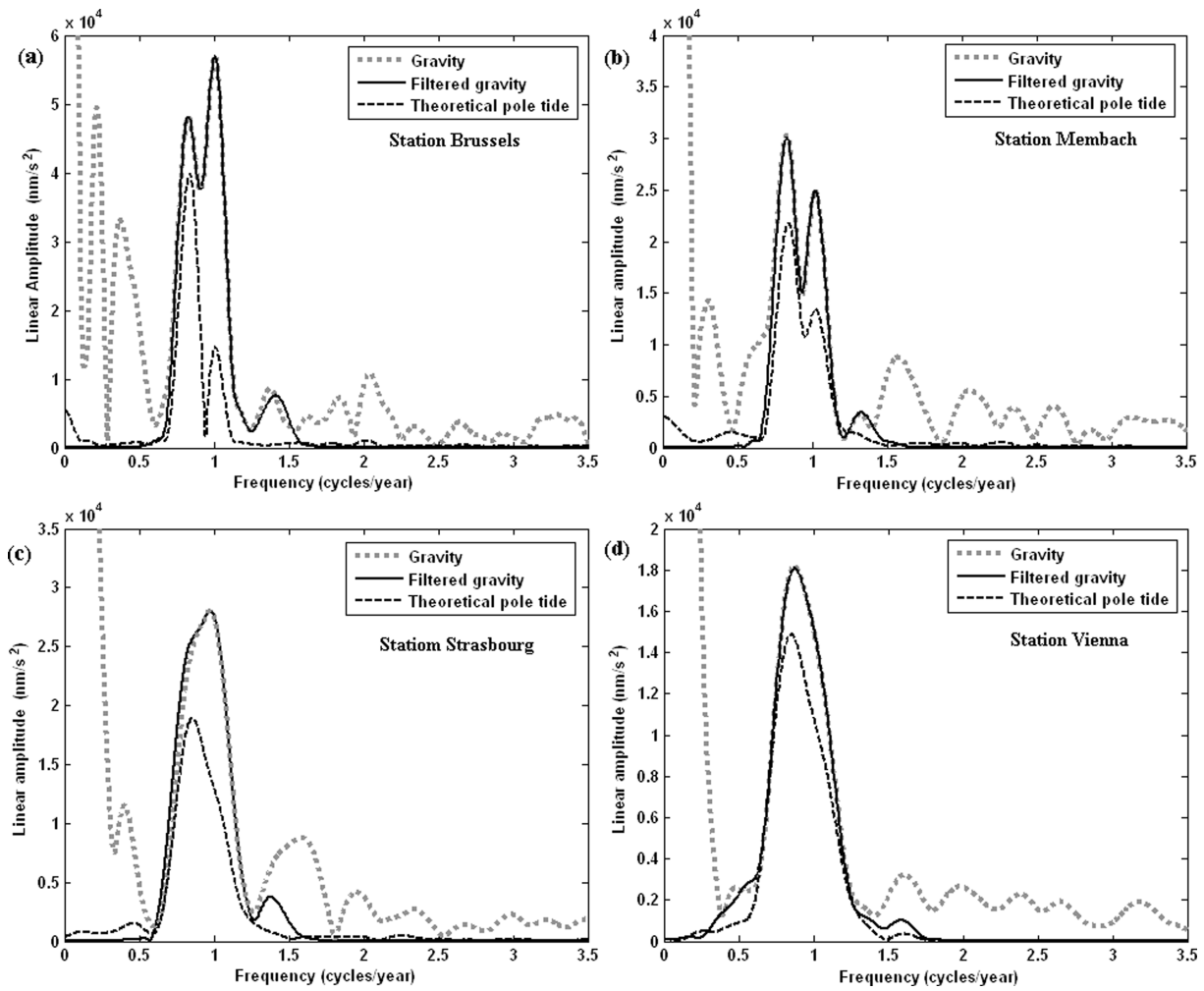


Figure 2. Wavelet filtering results for data series at station (a) Brussels, (b) Membach, (c) Strasbourg and (d) Vienna.



**Figure 3.** Comparison between the filtered and unfiltered gravity residuals in the frequency domain at station (a) Brussels, (b) Membach, (c) Strasbourg and (d) Vienna. The passband of the filter is  $0.713 \sim 1.426$  cpy (period band  $256 \sim 512$  d). These time-series are padded with zeros at their ends to length 65 536 and then multiply by Hanning windows before performing fast Fourier transform (FFT) to them.

while index  $i = 1, 2$  stands for the Chandler and annual component, respectively,  $P(t, \Delta T)$  is the local atmospheric pressure signal in the period range  $\Delta T = 256 \sim 512$  d, and  $C$  represents a value of barometric admittance, which is frequency-dependent.

Similarly the theoretical pole tide derived from eq. (4) is modelled as

$$\Delta g_2(t) = \sum_{i=1}^2 B_i \cos(\omega_i t + b_i). \quad (6)$$

We fit  $\Delta g_1$  to the observed pole tide  $\Delta G(t)$  (filtered gravity residual) and  $\Delta g_2$  to theoretical pole tide  $\Delta p$  (derived from eq. 4) by using the least-squares technique. After adjustment of the parameters  $A_i$ ,  $B_i$ ,  $a_i$  and  $b_i$ , amplitude factor  $\delta$  and phase difference  $\kappa$  at Chandler period can be estimated as:

$$\delta = A_1/B_1, \quad \kappa = a_1 - b_1. \quad (7)$$

Because in eq. (4) the observed polar motion is variable and  $\theta$  and  $\lambda$  are different at different stations, the Chandler frequency is not a constant for different stations and different epochs. In order to obtain the best fitting result, we select an optimum Chandler frequency by experimenting different  $\omega_1$  from 428 to 438 d step by 0.5 d until we find a minimum root mean squared (rms) value of the difference between the model  $\Delta p$  and the theoretical pole tide.

The optimum value, for example, at the station Membach is 431 d, and the corresponding minimum rms is about  $2.1 \text{ nms}^{-2}$ . Fig. 4 shows a good agreement between the sinusoidal functions and the pole tide at the station Membach. The value  $\delta$  and  $\kappa$  are  $1.1960 \pm 0.0119$  and  $0.6847 \pm 0.9126$ , respectively. The fitting results of the station Membach and of the three other stations are listed in Table 1.

## 5.2 Direct fit in the time domain

Because the Chandler wobble is not a pure harmonic, Chandler frequency is not a single value but a set of close frequencies. To avoid using a fixed Chandler frequency in the regression analysis, we try to fit directly the theoretical pole tide to SG records in the time domain. Since the Earth response to the long-period tide is not strongly frequency dependent, we may accept that amplitude factor  $\delta$  at the Chandler period is equal to that at annual period. For simplicity of model derivation, we mix up the annual terms of all different origin, except for annual wobble, in one sinusoidal expression (Ducarme *et al.* 2006), then the observed pole tide  $\Delta G(t)$  in the period band 256–512 d can be modelled as

$$\Delta g(t) = \delta \Delta p(t - \Delta t) + A \cos(\omega t + b) + C \cdot P(t, \Delta T), \quad (8)$$

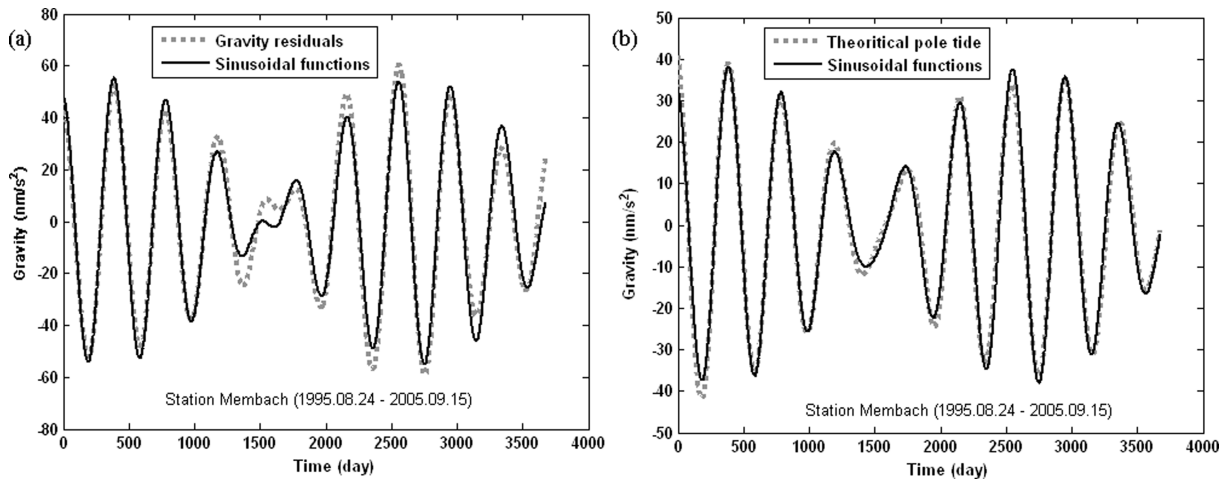


**Figure 4.** Fitting sinusoidal functions to the pole tide at the station Membach. (a) The best fit for the observed pole tide. (b) The best fit for the theoretical pole tide. The period band is 256 ~512 d and the length of the time-series is 3676 d.

**Table 1.** Results from different methods,  $\delta$ : Amplitude factor,  $\kappa$  ( $^\circ$ ): Phase difference (lag positive), Admittance in  $\text{nms}^{-2} \text{hPa}^{-1}$ , mean value: pressure admittance determined in the diurnal and semi-diurnal bands.

Station	Method	$\delta$	$\kappa$ ( $^\circ$ )	Pressure admittance
Brussels	<b>(a) This study</b> (13, Apr. 04, 1987 ~ 25, May 05, 2000)			
	Sinusoidal fit (435 d)	$1.1820 \pm 0.0338$	$-0.5967 \pm 2.0926$	2.84
	Fitting in the time domain	$1.1713 \pm 0.0067$	about $-2.52$	
	Fitting in the frequency domain	$1.1939 \pm 0.0294$	$-2.4088 \pm 1.4133$	
	<b>(b) Previous studies</b>			
	Xu <i>et al.</i> (2004) <sup>b</sup>	$1.1848 \pm 0.0504$	$-6.36 \pm 2.43$	2.81
	Harnisch & Harnisch (2006) <sup>b</sup>	$1.18 \pm 0.26$	$-8.3 \pm 11.0$	Mean value
Ducarme <i>et al.</i> (2006) <sup>a</sup>	$1.1865 \pm 0.0126$	about $-2.52$		
Membach	<b>(a) This study</b> (24, Aug, 1995 ~ 15, Sep., 2005)			
	Sinusoidal fit (431 d)	$1.1960 \pm 0.0119$	$0.6487 \pm 0.9126$	$-2.61$
	Fitting in the time domain	$1.1896 \pm 0.0084$	about 0.83	
	Fitting in the frequency domain	$1.2739 \pm 0.0019$	$0.6612 \pm 0.0848$	
	<b>(b) Previous studies</b>			
	Xu <i>et al.</i> (2004) <sup>b</sup>	$1.2613 \pm 0.0187$	$-4.97 \pm 0.85$	$-2.35$
	Harnisch & Harnisch (2006) <sup>b</sup>	$1.18 \pm 0.13$	about 2.4	Mean value
Ducarme <i>et al.</i> (2006) <sup>a</sup>	$1.1897 \pm 0.0137$	about 1.68		
Strasbourg	<b>(a) This study</b> (20, Apr., 1997 ~ 03, Jun, 2005)			
	Sinusoidal fit (435.5 d)	$1.1902 \pm 0.0157$	$4.3190 \pm 1.3261$	$-2.30$
	Fitting in the time domain	$1.1910 \pm 0.0030$	about 4.15	
	<b>(b) Previous studies</b>			
	Xu <i>et al.</i> (2004) <sup>b</sup>	$1.1767 \pm 0.0664$	$-27.04 \pm 3.23$	$-3.76$
	Harnisch & Harnisch (2006) <sup>b</sup>	$1.18 \pm 0.14$	about $-0.5$	Mean value
	Ducarme <i>et al.</i> (2006) <sup>a</sup>	$1.1856 \pm 0.0148$	about 1.68	
Vienna	<b>(a) This study</b> (21, Aug., 1997 ~ 2, Oct., 2004)			
	Sinusoidal fit (432 d)	$1.2092 \pm 0.0127$	$-5.7917 \pm 1.3345$	$-2.73$
	Fitting in the time domain	$1.2280 \pm 0.0082$	about $-4.98$	
	<b>(b) Previous studies</b>			
	Harnisch & Harnisch (2006) <sup>b</sup>	$1.20 \pm 0.13$	about 5.0	Mean value
Ducarme <i>et al.</i> (2006) <sup>a</sup>	$1.1526 \pm 0.0086$	about $-1.68$		

<sup>a</sup>Fitting in the time domain.

<sup>b</sup>Fitting at a fixed Chandler period of 432 d.

where  $\Delta p(t)$  is theoretical pole tide and  $\Delta t$  is time lag between the observed pole tide  $\Delta G(t)$  and the theoretical pole tide  $\Delta p(t)$ . The second term in eq. (8) is the model of environmental noise at annual frequency. The third term is the local atmospheric pressure effects, just as in eq. (5). The amplitude factor  $\delta$ , parameter  $A$ ,  $b$  and admittance  $C$  are estimated by fitting  $\Delta G(t)$  to the filtered gravity

residual  $\Delta G(t)$  with the least-square method at a optimum value of  $\Delta t$ . The optimum time lag  $\Delta t$  is determined by experimenting different values of  $\Delta t$  in the process of adjustment of  $A$ ,  $b$ ,  $C$  and  $\delta$  until we find a minimum rms value of the difference between  $\Delta G(t)$  and  $\Delta G(t)$ . Using this model we do not have to know the exact frequency of the Chandler wobble.



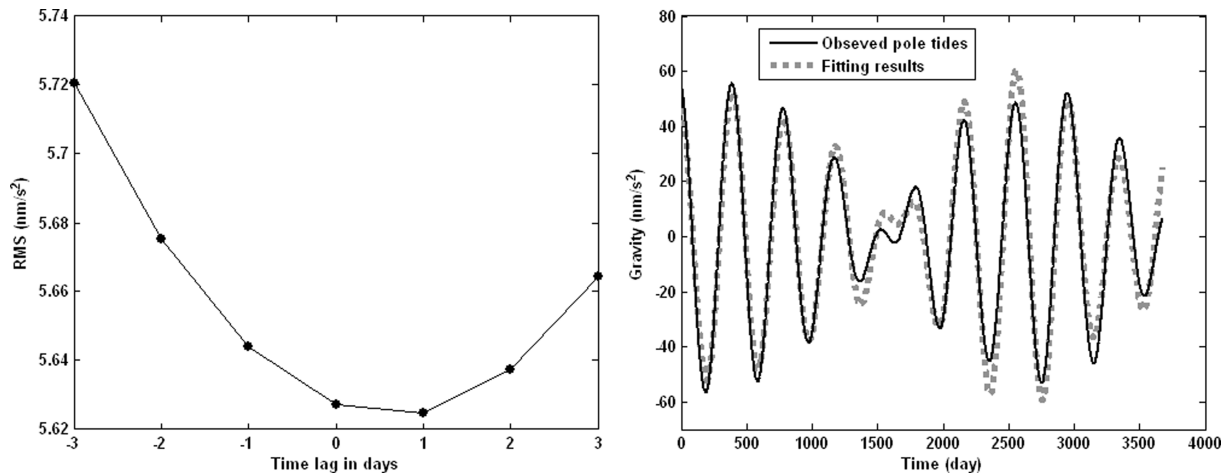


**Figure 5.** (a) Determination of optimum time lag  $\Delta t_{CH}$  by selecting the minimum rms between observed pole tides and theoretical ones. (b) The result of directly fitting theoretical tides to observed pole tides SG observations with time lag of a day. The period band is 256 ~ 512 d and the length of the data is 3676 d.

Fig. 5 shows the fit with a lag  $\Delta t_{CH}$  of a day and an example of determination of the optimum value for  $\Delta t$ . At the optimum value of one day shift, this method yields  $\delta = 1.1896 \pm 0.0084$  at station Membach. As the period of the Chandler wobble is around 432 d, one day shift corresponds to a phase lag about  $0.83^\circ$ . Compared to the results derived from the sinusoidal fitting method, the amplitude factor  $\delta$  agrees within the mean square deviation (MSD) but the precision is much improved (see Table 1).

### 5.3 Fit in the frequency domain

According to Fourier analysis theory, at least 6.5 yr long time-series is necessary to separate the Chandler component from the annual one in the frequency domain with a rectangular window. We can see from Fig. 3 that with the Hanning window the spectrum peak at the annual frequency is partly separated from that at the Chandler frequency for data from Brussels and Membach. The rectangular window can provide better resolution of gravity spectra if its spectral leakage is suppressed. To reduce spectral leakage of in the Discrete Fourier transform, we removed large long-period components by wavelet

filtering before performing Fourier transform. Fig. 6 shows that two peaks are almost totally separated by using rectangular windows. After wavelet filtering gravity residuals, the spectral leakage of the rectangular window is only a little bit larger than that of the Hanning-window, but the resolution of spectrum is much improved (compare it with Figs 3a and b).

We try to estimate the amplitude factor  $\delta$  and phase difference  $\kappa$  of Chandler wobble in the frequency domain. The gravimetric factor is defined in the frequency domain as:

$$\tilde{\delta}(f) = \frac{G(f)}{P(f)}, \tag{9}$$

where  $f$  represents frequency,  $G(f)$  and  $P(f)$  are the discrete Fourier transform of the observed pole tides and of the theoretical pole tides, respectively. Thus the factor  $\tilde{\delta}(f)$  is a complex scalar, namely,  $\tilde{\delta}(f) = \delta e^{-i\kappa}$ , where  $\delta$  is amplitude factor and  $\kappa$  is phase difference between  $G(f)$  and  $P(f)$ . The linear regression transfer function is performed as

$$\Delta G(f) = G(f) - \tilde{\delta}(f)P(f). \tag{10}$$

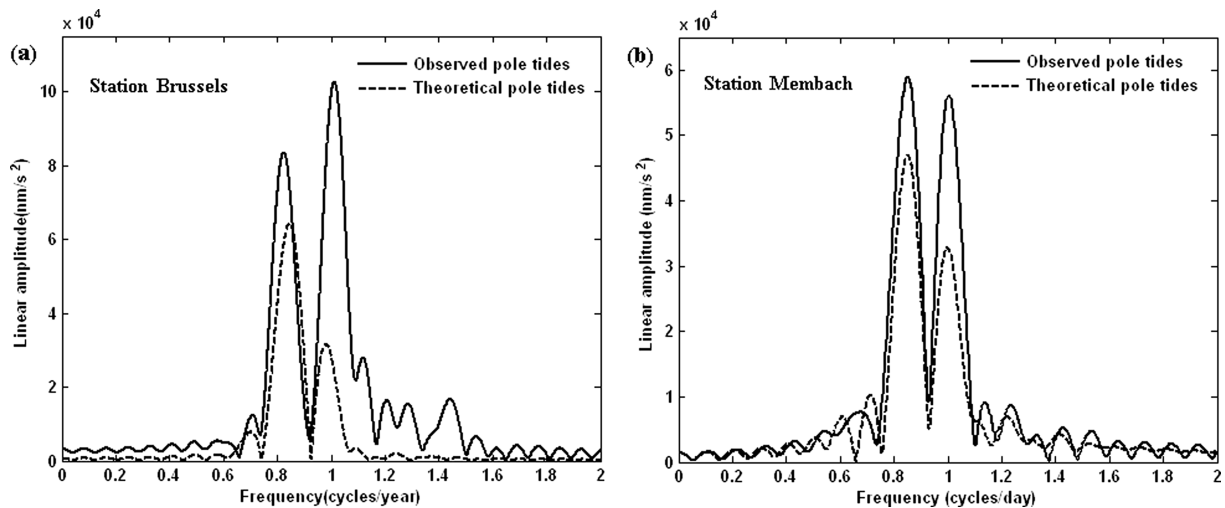


**Figure 6.** Discrete Fourier transform of pole tides at the station Brussels (a) and Membach (b), now with rectangular window. Prior to FFT the data is padded with zeros from 4792 (Brussels) and 3676 (Membach) to 65 536 points, and large long-term components are filtered out in order to reduce spectral leakage.

Minimizing  $|\Delta G(f)|^2$  in a least squares sense over a narrow frequency range  $f = 1/440 \sim 1/424$  cpd lead to

$$\delta(f) = \frac{\sum [G(f)\tilde{P}(f)]}{\sum |P(f)|^2} \quad (11)$$

The real and imaginary solutions are

$$\delta_R = \frac{\sum [G_R(f)P_R(f) + G_I(f)P_I(f)]}{\sum |P(f)|^2} \quad (12)$$

$$\delta_I = \frac{\sum [G_I(f)P_R(f) - G_R(f)P_I(f)]}{\sum |P(f)|^2}. \quad (13)$$

These can be combined into the amplitude factor  $\delta = \sqrt{\delta_R^2 + \delta_I^2}$  and phase difference  $\kappa = \arctg(\delta_I/\delta_R)$ . With a rectangular window, we obtain  $\delta = 1.1939 \pm 0.0294$ ,  $\kappa = -2.4088^\circ \pm 1.4133$  at the station Brussels and  $\delta = 1.2739 \pm 0.0019$ ,  $\kappa = 0.6612^\circ \pm 0.0848$  at the station Membach. Note that it is the first time that Fourier transform is used in pole tide analysis. The amplitude factors obtained in the frequency domain are obviously larger than values we just obtained in the time domain. It is mainly due to the fact that observed pole tides at Brussels and Membach have some components which are not included in theoretical pole tides.

## 6 RESULTS AND DISCUSSIONS

Wavelet filtering method based on Daubechies wavelet shows advantage in analysis of long-term gravity variations in gravimetric time-series. Table 1 gives a summary of our results and a comparison with previous results from different authors. In most cases, although the estimated  $\delta$ -factors agree within their associated MSD, it is clear that the rms errors derived from this study are significantly smaller than those from previous studies, which means that our results are more reliable. Our estimation yields higher internal precision mainly because wavelet filtering method eliminates effectively the instrumental drift and provides smoothed data series for the regression analysis. As a matter of fact, the wavelet method removes all constituents outside the period range 256–512 d, including not only the instrumental drift but also real long-term constituents of other origins. Absolute gravity measurements are no more required to support the drift modelling.

The estimated  $\kappa$ -values of different methods are quite scattered in Table 1. We infer that some unreasonable  $\kappa$ -values may be due to the method itself. There is a reasonable agreement between Ducarme *et al.* (2006) and this study.

It has been usually believed that at low frequency the local barometric pressure cannot be used to adequately remove the long-period

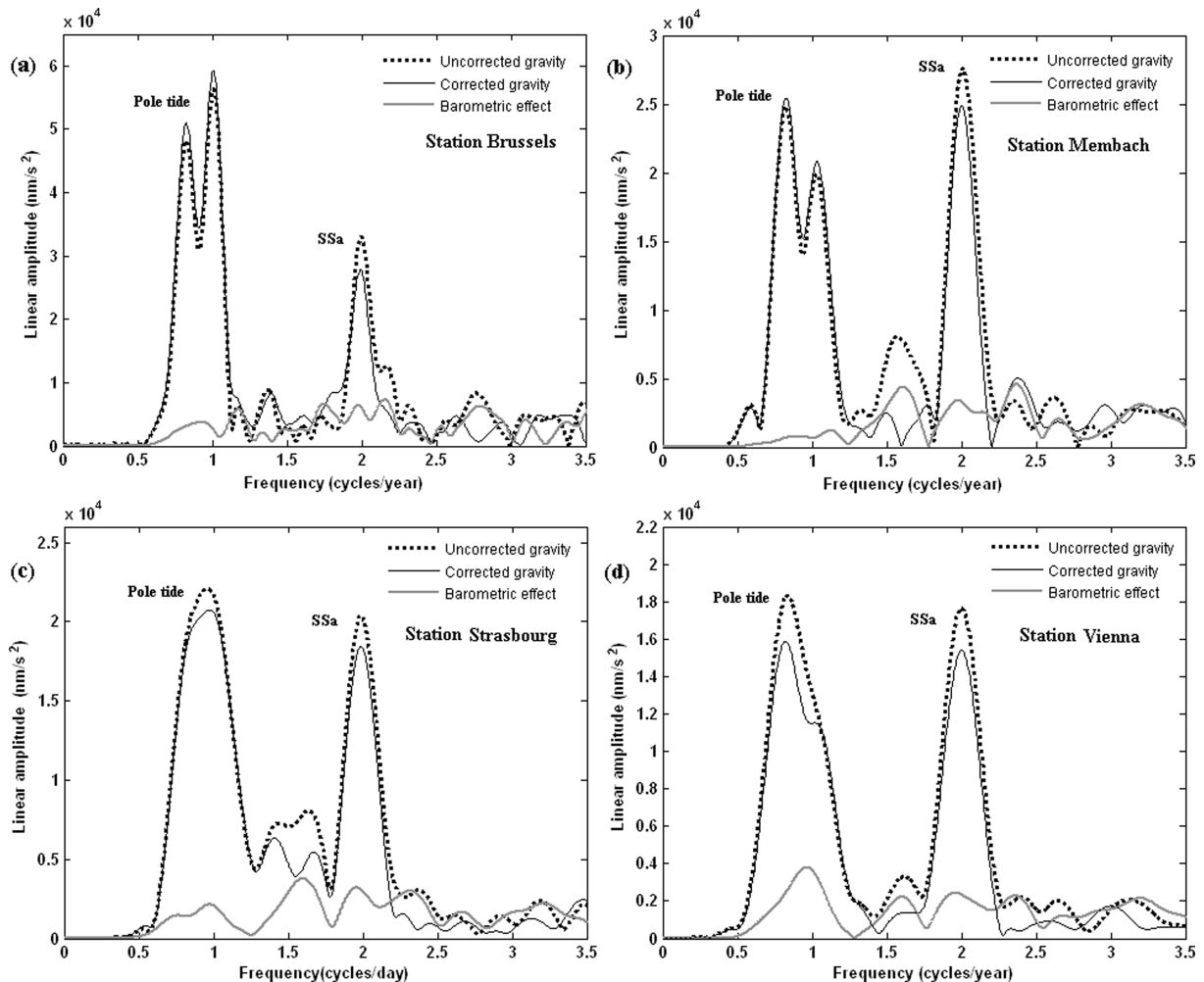


**Figure 7.** Gravity variations before and after local pressure corrections (with admittances in Table 1). The barometric effect is the local barometric data multiplied by a barometric admittance. The long-period term of gravity variation is eliminated by wavelet filtering. The Hanning-window is used before performing FFT.

air pressure effect, as the pressure cells have a regional extension. However, it is not really the case, Boy *et al.* (2002) showed that the global 3-D atmospheric loading modelling allows a significant reduction of gravity residuals versus the correction using local barometric admittance. However, this reduction is effective only between about 5 and 100 d. For longer periods, the global pressure correction does not show better improvement than local pressure correction in term of reduction of the variance of gravity residuals. It is a reason why the local pressure correction is still used in this study for the pole tide analysis.

Barometric admittance values (see Table 1), estimated in the period band 256–512 d by least-squares adjustment in the ‘fitting-in-the-time-domain method’, are obviously smaller than their corresponding mean values over the whole frequency band, that is, about  $-3.467$ ,  $-3.303$ ,  $-3.02$  and  $-3.532$   $\text{nms}^{-2}$   $\text{hPa}^{-1}$  at the station Brussels, Membach, Strasbourg and Vienna, respectively. Local atmospheric pressure corrections with frequency-dependent admittances can avoid injecting extra noise in the pole tide band.

Fig. 7 shows spectra of surface gravity variations for four stations before any atmospheric correction, and with local atmospheric corrections. Barometric effects, derived from local barometric measurement multiplied by admittances in Table 1, are also showed in Fig. 7. Local atmospheric correction allows an obviously reduction of gravity variation at the station Strasbourg and Vienna. For SGs at the station Brussels and Membach, however, spectral amplitudes at the annual and Chandler frequency are somewhat increased after the correction. This phenomenon may be mainly due to the large scale elastic deformation caused by ocean loading, as the two stations are very close to the Northern sea.

For long-period solid-Earth tides, Earth response models, such as DDW99 (Dehant *et al.* 1999), show that the amplitude factor should be close to 1.16 and that the phase difference could be a very small lag due to mantle anelasticity. However, in this study all the amplitude factors at the four stations are comparatively large ( $\delta > 1.18$ ) and some phase lags differ considerably from zero. In an earlier study Boy *et al.* (2000) pointed out the fact that the indirect effect of the ocean pole tide could increase the amplitude factor up to 1.185 in Western Europe. This fact was confirmed by Ducarme *et al.* (2006) who found a mean amplitude factor  $\delta = 1.1788 \pm 0.0040$  for nine GGP stations. After correction of the ocean pole tide effect the value becomes 1.1605. Harnisch & Harnisch (2006) found out that hydrological influences significant affect  $\delta$ - and  $\kappa$ -values. Due to the high quality data at the four stations and the advantage of wavelet method the estimated pole tidal parameters are reliable and thus confirm their investigation indirectly.

Among the three regression analysis methods used for pole tide analysis, we recommend the ‘fitting-in-the-frequency-domain’ method, on condition that the time-series is long enough for the safe separation of the Chandler component from the annual one in the frequency domain. The reason is that this method does not need a fixed Chandler period, can assign uncertainties to estimates of  $\delta$ - and  $\kappa$ -values and yields a comparatively low MSD. The disadvantage of the ‘fitting-in-the-time-domain method’ is that it cannot assign uncertainty on the estimated  $\kappa$ -values. Concerning the sinusoidal fitting method, it is impossible to fit two sinusoidal functions to a very long time-series of the pole tide.

Wavelet filtering contributes to improve pole tide analysis by efficiently eliminating noise in SG records. However, environmental noise at the pole tidal band cannot be removed by wavelet method. To achieve further improvement, long-period environmental effects, such as the global ocean loading, the influence of underground and

superficial water, should be removed by introduced more auxiliary data and environmental mathematical models.

## ACKNOWLEDGMENTS

We are grateful to the GGP-cooperation for providing valuable data at the selected stations. This study is financed by the National Natural Sciences Foundation of China (grant No. 40574009) and Chinese Academy of Sciences (CAS) Hundred Talent Program.

## REFERENCES

- Boy, J.-P., Hinderer, J., Amalvict, M. & Calais, E., 2000. On the use of long records of superconducting and absolute gravity observations with special application to the Strasbourg station, France. *Cahiers Centre Europ. Géodyn. Séismol.*, **17**, 67–83.
- Boy, J.P., Gegout, P. & Hinderer, J., 2002. Reduction of surface gravity from global atmospheric pressure loading, *Geophys. J. Int.*, **149**(2), 534–545.
- Capitaine, N., 1986. The earth rotation parameters: conceptual and conventional definitions, *Astr. Astrophys.*, **162**, 323–329.
- Crossley, D., Jensen, O. & Hinderer, J., 1995. Effective atmospheric admittance and gravity residuals, *Phys. Earth. planet. Inter.*, **90**, 221–241.
- Crossley, D. *et al.*, 1999. Network of superconducting gravimeters benefits a number of disciplines, *EOS, Trans. Am. geophys. Un.*, **80**(11), 121–126.
- Daubechies, I., 1988. Orthonormal Bases of Compactly Supported Wavelet, *Commun Pure Appl Math.*, **41**, 909–996.
- Daubechies, I., 1992. *Ten Lectures on Wavelets*, in Number 61 in *CBMS-NSF Series in Applied Mathematics*, SIAM, Philadelphia.
- Dehant, V., Defraigne, P. & Whar, J., 1999. Tides for a convective Earth, *J. geophys. Res.*, **104**(B1), 1035–1058.
- De Meyer, F. & Ducarme, B., 1991. Non-tidal gravity changes observed with a superconducting gravimeter, in *Proc 11th Int Symp on Earth tides*, pp. 167–184, eds Kakkuri, J., Helsinki, Schweizerbastische Verlagsbuchhandlung, Stuttgart.
- Ducarme, B., van Ruymbeke, M., Venedikov, A.P., Arnos, J. & Vieira, R., 2005. Polar motion and non tidal signals in the superconducting gravimeter observations in Brussels, *Bull. Inf. Marées Terrestres*, **140**, 1153–1171.
- Ducarme, B., Venedikov, A.P., Arnos, J., Chen, X.-D., Sun, H.-P. & Vieira, R., 2006. Global analysis of the GGP superconducting gravimeters network for the estimation of the pole tide gravimetric amplitude factor, *J. Geodyn.*, **41**, 334–344.
- Harnisch, M. & Harnisch, G., 2006. Study of long-term gravity variations, based on data of the GGP Co-operation, *J. Geodyn.*, **41**, 318–325.
- Hinderer, J. & Legros, H., 1989. Elasto-gravitational deformation relative gravity changes and earth dynamics, *Geophys. J.*, **97**, 481–495.
- Hu, X.-G., Liu, L.-T., Hinderer, J. & Sun, H.-P., 2005. Wavelet filter analysis of local atmospheric pressure effects on gravity variations, *J. Geodyn.*, **79**(8), 447–459.
- Hu, X.-G., Liu, L.-T., Hinderer, J., Hsu, H.T. & Sun, H.-P., 2006a. Wavelet filter analysis of atmospheric pressure effects in the long-period seismic mode band, *Phys. Earth. planet. Inter.*, **154**, 70–84.
- Hu, X.-G., Liu, L.-T., Ducarme, B., Hsu, H.T. & Sun, H.-P., 2006b. Wavelet filter analysis of local atmospheric pressure effects in the long-period tidal bands, *Phys. Earth. planet. Inter.*, **159**, 59–70.
- Kaneko, Y., Sato, T. & Sasao, T., 1974. Periodic variation of earth’s gravity due to the polar motion and possibility of its observational detection by means of absolute gravimeter, *Proc. Int. Latit. Obs. Mizusawa*, **14**(14), 24–25.
- Loyer, S., Hinderer, J. & Boy, J., 1999. Determination of the gravimetric factor at the Chandler period from Earth’s orientation data and superconducting gravimetry observations, *Geophys. J. Int.*, **136**, 1–7.
- Mallat, S., 1989a. Multiresolution approximations and wavelet orthonormal bases of  $L_2(\mathbb{R})$ , *Trans Amer Math Soc*, **315**, 69–87.



- Mallat, S., 1989b. A theory for multiscale signal decomposition: the wavelet representation, *IEEE Trans Pattern Anal. Machine Intell.*, **11**, 674–693.
- Neumeyer, J., 1995. Frequency-dependent atmospheric pressure correction on gravity variations by means of cross spectral analysis, *Bull. Inf. Marées Terrestres*, **122**, 9212–9220.
- Richter, B. & Zürn, W., 1988. Chandler effects and the nearly diurnal free wobble as determined from observations with a superconducting gravimeter, in *The Earth's Rotation and Reference Frames for Geodesy and Geodynamics*, pp. 309–315, eds Babcock, A. & Wilkins, G., Kluwer, Dordrecht.
- Richter, B., Wenzel, H.-G., Zürn, W. & Klopping, F., 1995. From Chandler wobble to free oscillations: comparison of cryogenic gravimeters and other instruments over a wide period range, *Phys. Earth planet. Int.*, **91**, 131–148.
- Sato, T., Ooe, M., Nawa, K., Shibuya, K., Tamura, Y. & Kaminuma, K., 1997. Long-period tides observed with a superconducting gravimeter at Syowa station, Antarctica, and their implication to global ocean tide modeling, *Phys. Earth planet. Int.*, **103**, 39–53.
- Sato, T., Fukuda, Y., Aoyama, Y., McQueen, H., Shibuya, K., Tamura, Y., Asari, K. & Ooe, M., 2001. On the observed annual gravity variation and the effect of sea surface height variations, *Phys. Earth planet Int.*, **123**, 45–63.
- Tamura, Y., 1987. A harmonic development of the tidal-generating potential, *Mar Terrest Bull d'Info*, **99**, 6813–6855.
- Van Camp, M. & Vauterin, P., 2005. Tsoft: graphical and interactive software for the analysis of time series and Earth tides, *Comput. Geosci.*, **31**(5), 631–640.
- Venedikov, A.P., Arnosó, J. & Vieira, R., 2001. Program VAV/2000 for tidal analysis of unevenly spaced data with irregular drift and colored noise, *J. Geodetic Soc. Jpn.*, **47**(1), 281–286.
- Venedikov, A.P., Arnosó, J. & Vieira, R., 2003. VAV: a program for tidal data processing, *Comput. Geosci.*, **29**, 487–502.
- Vauterin, P., 1988. Tsoft: graphical and interactive software for the analysis of Earth's tides, Imprimerie Robert Louis, Bruxelles, 481–486.
- Wahr, J.M., 1985. Deformation induced by polar motion, *J. geophys. Res.*, **90**(B11), 9363–9368.
- Xu, J.Q., Sun, H.P. & Yang, X.F., 2004. A study of gravity variations caused by polar motion using superconducting gravimeter data from the GGP network, *J. Geodyn.*, **38**, 201–209.